Measurements of Bubble-Point Pressures and Liquid Densities of Binary Mixtures: Trifluoromethyl Methyl Ether (HFE-143m) + 1,1,1,2-Tetrafluoroethane (HFC-134a), and Trifluoromethyl Methyl Ether (HFE-143m) + Pentafluoroethane (HFC-125)

J. V. Widiatmo,* Y. Morimoto, and K. Watanabe

Department of System Design Engineering, Faculty of Science and Technology, Keio University, 3-14-1, Hiyoshi, Kohoku-ku, Yokohama 223-8522, Japan

Measurements of the bubble-point pressures and the liquid densities of the binary mixtures trifluoromethyl methyl ether (CF_3OCH_3, HFE-143m) + 1,1,1,2-tetrafluoroethane (CF_3CH_2F, HFC-134a) and HFE-143m + pentafluoroethane (CF_3CHF_2, HFC-125) at temperatures from (280 to 360) K are reported. The measurements were performed using a magnetic densimeter coupled with a variable volume cell with uncertainties being ±8 mK in temperature, ±2 kPa in pressure for the single phase, ±12 kPa in bubble-point pressure, and ±2.2 kg·m^{-3} in density. The measured bubble-point pressures have been used in the present study to optimize the binary interaction parameter of the Peng−Robinson equation of state. On the basis of the measured liquid densities and bubble-point pressures, a compressed-liquid density correlation has also been developed, which led to a satisfactory representation within ±2.2 kg·m^{-3} in the liquid phase.

Introduction

In accord with an increasing concern about global warming, the Research Institute of Innovative Technology for the Earth (RITE), Kyoto, Japan, has proposed hydrofluoroethers (HFEs), which have zero ozone depletion potential (ODP) and significantly low global warming potential (GWP), as promising new generation alternative refrigerants. Related earlier studies include those by Wang et al.[1] and by Salvi-Narkhede et al.,[2] who reported measurements of vapor pressures, liquid molar volumes, and critical properties of some fluorinated ethers. Sako et al.[3,4] published vapor pressure and critical property measurements of fluorinated ethers proposed by the RITE. Studies of the fluorinated ether mixtures include those by Beyerlein et al.,[5] who reported vapor pressures and bubble-point pressures of several mixture systems including fluorinated ethers. Kul et al.[6,7] conducted vapor pressure measurements for some pure fluorinated ethers and bubble-point pressure measurements for several HFE mixtures with ethane derivative HFCs using the same apparatus used by Beyerlein et al.[2]

Among the proposed candidates by RITE, trifluoromethyl methyl ether (CF_3OCH_3, HFE-143m) is considered as a promising candidate to replace dichlorodifluoromethane (CCl_2F_2, R-12) and could be a replacement for HFC-134a (CF_3CH_2F) being conventionally used for refrigeration system applications. Yamada et al.,[8] however, reported the flammability measurements for HFE-143m along with its thermal stability and toxicity. From their measurements, it is found that, besides being thermally stable and having lower toxicity, HFE-143m has slight flammability. We, therefore, consider possible blends of HFE-143m with HFC-134a and HFC-125 so as to create mixture refrigerants with much lower flammability that are still thermodynamically promising. The present paper aims to provide accurate results for bubble-point pressures and liquid densities of the binary HFE-143m + HFC-134a and HFE-143m + HFC-125 mixtures. Optimization of the Peng−Robinson (PR) equation of state[9] that enables a reliable bubble-point pressure data representation will be discussed. Development of a compressed-liquid density correlation to reproduce the measured liquid densities is also presented. The basic thermodynamic properties of HFE-143m, HFC-134a, and HFC-125 are given in Table 1.

Table 1. Basic Thermodynamic Properties of HFC-134a and HFE-143m

	HFC-134a[a]	HFC-125[a]	HFE-143m
T_c/K	374.11	339.17	377.901[b]
P_c/kPa	4052	3620	3640[c]
ρ_c/kg·m^{-3}	508	577	464[b]
M/kg·kmol^{-1}	102.03	120.022	100.04
ω	0.327	0.305	0.267
T_b/K	247.062[d]	225.028[d]	249.486[d]

[a] Widiatmo et al.[10] [b] Yoshii et al.[11] [c] Widiatmo et al.[12] [d] From the PR equation.

Experimental Studies

A magnetic densimeter coupled with a variable volume cell has been used in the present study to measure liquid densities of the binary HFE-143m + HFC-134a and HFE-143m + HFC-125 mixtures. The experimental apparatus is shown in Figure 1. The apparatus consists of a temperature control and measurement section, a pressure control and measurement section, and a density measurement section. The temperature is determined by means of a 25 Ω platinum resistance thermometer (R) placed in the

* To whom correspondence should be addressed.

10.1021/je020055b CCC: $22.00
Published on Web 08/14/2002

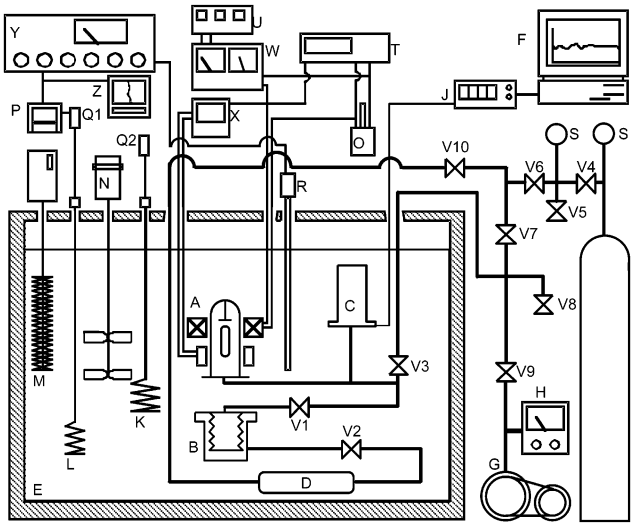

Figure 1. Experimental apparatus: A, magnetic densimeter; B, variable volume cell; C, digital quartz pressure transducer; D, damper; E, thermostated fluid bath; F, personal computer; G, vacuum pump; H, vacuum gauge; I, nitrogen gas; J, digital quartz pressure computer; K, main heater; L, subheater; M, cooler; N, stirrer; O, standard resistor; P, PID controller; Q1, Q2, thyristor transformer; R, 25 Ω standard platinum resistance thermometer; S, pressure gauge; T, digital multimeter; U, current controller; V1−V10, valves; W, dc power supply; X, galvanometer; Y, thermometer bridge; Z, pen recorder.

vicinity of the magnetic densimeter (A) immersed in a thermostated fluid bath (E). The pressure is measured using a quartz pressure transducer (C), while the density is obtained from the magnetic densimeter. By combining the magnetic densimeter with the variable volume cell (B), it is possible to create a vapor−liquid coexisting state or a compressed-liquid phase within the sample. The bubble-point condition is determined from careful visual observation of the appearance and disappearance of a bubble in the sample. In the case of mixtures, the mixture composition is determined through weighing the supply vessels before and after condensing the sample into the variable volume cell. Detailed explanations of the present apparatus as well as experimental procedures have been reported elsewhere.[13]

Through the procedure adopted in the present study, the temperature, pressure, and density measurements can be performed within the uncertainties of ±8 mK, ±2 kPa, and ±2.2 kg·m^{-3}, respectively, according to the ISO recommendation[14] in terms of the expanded uncertainties with a coverage factor of 2. The uncertainty in the bubble-point pressure measurements is estimated to be ±12 kPa, considering ±10 kPa as the additional uncertainty in determining the disappearance of the minute bubble from the liquid phase. The uncertainty in mixture composition is estimated to be not greater than ±0.3 mass %. Analyses of our sample purities by the manufacturers resulted in 99.4 mass % for HFE-143m, 99.95 mol % for HFC-134a, and 99.9 mass % for HFC-125. No further purification has been done in the present study, except degassing with the aid of liquefied nitrogen more than eight times for HFE-143m before the measurements.

Results and Discussion

Bubble-point pressures of the binary HFE-143m + HFC-134a and HFE-143m + HFC-125 mixtures have been measured at temperatures from (280 to 350) K in 10 K intervals and mole fractions of 0.25, 0.50, and 0.75 HFE-143m. The numerical values of the measured bubble-point pressures are tabulated in Tables 2 and 3, where x_1 denotes the mole fraction of HFC-143m as the first component.

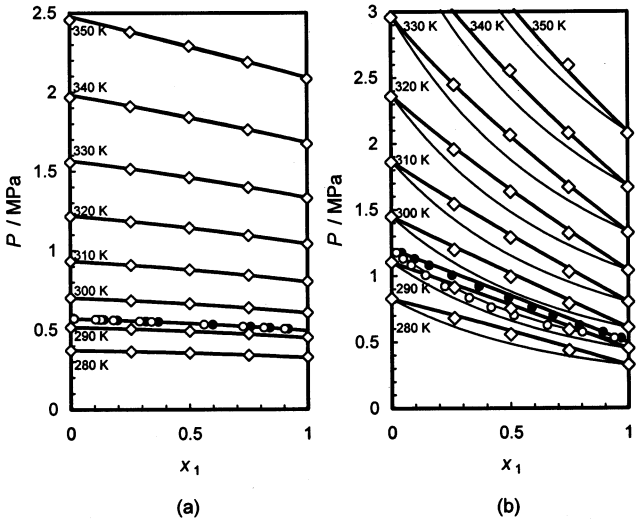

Figure 2. Distribution of the measured bubble-point pressures of the binary HFE-143m + HFC-134a mixture (a), and the binary HFE-143m + HFC-125 mixture (b): ◇, this work; ●, bubble-point by RITE;[15] ○, dew-point by RITE.[15]

Table 2. Bubble-Point Pressures of the Binary HFE-143m (1) + HFC-134a (2) System

	T	*P*		*T*	*P*
x_1	K	kPa	x_1	K	kPa
0.7504	279.989	340.4	0.5012	319.986	1141.9
0.7504	289.988	473.4	0.5012	329.985	1458.9
0.7504	299.987	639.2	0.5012	339.985	1839.8
0.7504	309.986	843.7	0.5012	349.984	2290.2
0.7504	319.986	1094.3	0.2546	279.989	362.5
0.7504	329.985	1396.5	0.2546	289.988	505.7
0.7504	339.985	1760.5	0.2546	299.987	685.0
0.7504	349.984	2188.4	0.2546	309.986	908.2
0.5012	279.989	354.2	0.2546	319.986	1181.3
0.5012	289.988	491.9	0.2546	329.985	1512.3
0.5012	299.987	665.3	0.2546	339.985	1908.8
0.5012	309.986	879.5	0.2546	349.984	2379.6

Table 3. Bubble-Point Pressures of the Binary HFE-143m (1) + HFC-125 (2) System

	T	*P*		*T*	*P*
x_1	K	kPa	x_1	K	kPa
0.7474	279.989	434.2	0.5008	309.986	1289.3
0.7474	289.988	591.8	0.5008	319.986	1633.8
0.7474	299.987	789.7	0.5008	329.985	2064.0
0.7474	309.986	1029.6	0.5008	339.985	2552.8
0.7474	319.986	1320.0	0.2647	279.989	679.4
0.7474	329.985	1669.1	0.2647	289.988	912.3
0.7474	339.985	2077.7	0.2647	299.987	1197.3
0.7474	349.984	2593.7	0.2647	309.986	1541.7
0.5008	279.989	556.9	0.2647	319.986	1954.9
0.5008	289.988	751.1	0.2647	329.985	2446.5
0.5008	299.987	992.3			

The data distribution of the bubble-point pressures of the binary HFE-143m + HFC-134a and HFE-143m + HFC-125 mixtures is illustrated in parts a and b, respectively, of Figure 2. Solid bold lines in this figure show the bubble-point pressures calculated from the PR equation discussed below, which is optimized on the basis of the experimental data and is used to calculate the respective dew-point pressures, shown in the figures by solid thin lines. The solid thin lines in Figure 2a are almost indistinguishable, since the calculated bubble-point and dew-

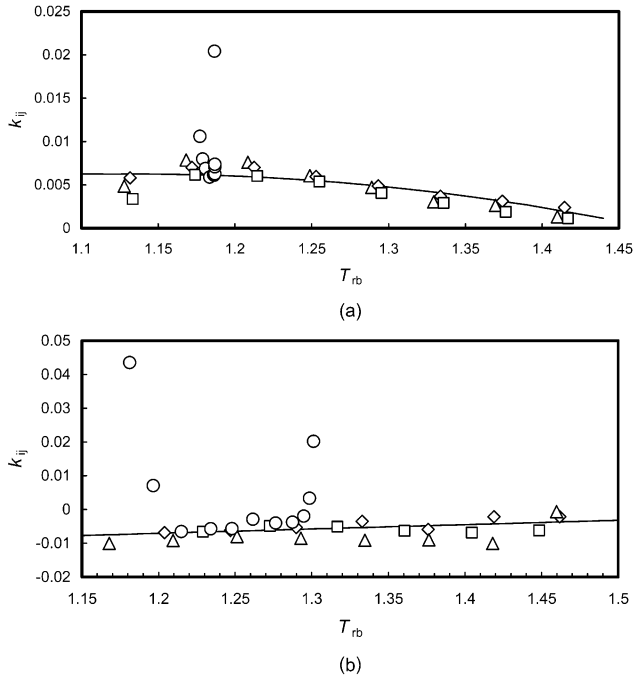

Figure 3. Temperature dependence of k_{ij} of the binary HFE-143m + HFC-134a mixture (a), and the binary HFE-143m + HFC-125 mixture (b): △, this work (0.75 mol of HFE-143m); ◇, this work (0.50 mol of HFE-143m); □, this work (0.25 mol of HFE-143m); ○, RITE.[15]

point pressures are almost overlapping; they appear nearly as a single curve for each isotherm. This shows that the binary HFE-143m + HFC-134a system is a near azeotrope and it obeys Raoult's law, since the bubble-point pressure curve forms nearly a straight line. On the contrary, the bubble-point pressures of the binary HFE-143m + HFC-125 mixture appear clearly as separate curves from their corresponding dew-point pressures, as shown in Figure 2b. The figure confirms clearly that the binary HFE-143m + HFC-125 mixture is zeotropic, since there is no overlapping of the curves, but it still obeys Raoult's law. Also shown in Figure 2 are the vapor−liquid equilibrium (VLE) data by the RITE,[15] which visually show agreement with the calculated bubble-point and dew-point pressures.

The PR equation, whose parameters are tabulated in Table 1, is used to represent the measured bubble-point pressures. A binary interaction parameter of the PR equation, k_{ij}, is included in the mixing rule for the term expressing the attraction of different molecules. This k_{ij} is usually considered as a fitting parameter for the VLE properties of mixtures, with which a rational thermodynamic property representation may be derived in a wider temperature range where no available data exist. In the present study, the k_{ij} is found to be dependent on temperature. Parts a and b, respectively, of Figure 3 illustrate the temperature dependence of the k_{ij} for the binary HFE-143m + HFC-134a and HFE-143m + HFC-125 mixtures. A reduced temperature against a normal boiling-point temperature, $T_{rb} = T/T_b$, has been chosen in these figures so as to obtain "a same fluid condition" in comparing the k_{ij} values at various compositions. The normal boiling-point temperature, T_b, has been adopted as the reducing temperature to replace the conventional critical temperature simply because of the reason that the critical temperature locus of the mixtures was unsuccessfully derived from the PR equation in the present study. Moreover, the available bubble-point pressures exist at temperatures very near the

Table 4. Cross Parameters Used in Eqs 1 and 5

	HFE-143m + HFC-134a	HFE-143m + HFC-125
$2\Delta T_{cij}$/K	−3.142	4.162
$2\Delta P_{cij}$/MPa	−0.090	0.309
$2\Delta v_{cij}$/(cm^3·mol^{-1})	26.316	3.253
$2\Delta\omega_{ij}$	0.024	−0.234
$2\Delta T_{b12}$/K	−3.4524	−18.836
$2\Delta a_{ij}$	0.056	0.1266
$2\Delta b_{ij}$	−0.247	−0.05771
$2\Delta A_{ij}$	1.148	0.8947
$2\Delta B_{ij}$	−0.867	−1.192

normal boiling-point of the mixtures, so that, to some extent, a reliable normal boiling-point temperature value would possibly be derived. The derived normal boiling temperature locus of the binary mixtures, T_b, can be expressed by eq 1. The first coefficient, T_{b1}, on the right-hand side of eq 1 shows the normal boiling-point temperature of the first component, while T_{b2} is that of the second component and ΔT_{b12} is the temperature deviation from the mole averaged boiling-point temperature. Their numerical values are tabulated in Tables 1 and 4. It should be noted that the assumption $k_{12} = k_{21}$ has been adopted in the present study for simpler k_{ij} optimization.

$$T_b = T_{b1}x_1 + T_{b2}(1 - x_1) + 2\Delta T_{b12}x_1(1 - x_1) \qquad (1)$$

The temperature dependence of k_{ij} shown in Figure 3a by a solid curve for the binary HFE-143m + HFC-134a mixture indicates k_{ij} values decrease with increasing temperature, which is then represented by eq 2 in the present study. Two data points (open circle) in the figure showing significant offset are those for the RITE data[15] near the pure components, and they have been excluded in the optimization. It should be emphasized that eq 2 is only valid at temperatures where the data exist, that is, from (280 to 350) K. Although there are no reported data, Figure 3a may imply that below 280 K ($T_{rb} < 1.13$) the k_{ij} would likely be constant with a value of 6.24×10^{-3}.

$$k_{ij} = -0.0641 + 0.1240T_{rb} - 0.0546T_{rb}^2 \qquad (2)$$

Concerning the binary HFE-143m + HFC-125 mixture as shown in Figure 3b, the k_{ij} increases linearly with increasing temperature, at least at the temperatures $T_{rb} > 1.16$. The k_{ij} showing significant positive values (open circle) were those optimized on the basis of the RITE data[15] at compositions near the pure components. Even if we exclude those compositions near the pure components, the k_{ij} based on the RITE data[15] also shows clearly the temperature dependence. Such temperature dependence has been expressed in the present study by a functional form given in eq 3, as shown by a solid straight line in Figure 3b.

$$k_{ij} = -0.02306 + 0.01328T_{rb} \qquad (3)$$

Parts a and b, respectively, of Figure 4 depict the deviation of the measured bubble-point pressures of the binary HFE-143m + HFC-134a and HFE-143m + HFC-125 mixtures, respectively, from the PR equation mentioned above. A satisfactory bubble-point pressure representation within ±3.5 kPa, which is even better than the estimated experimental uncertainty, has been obtained for the binary HFE-143m + HFC-134a mixture, while, for the binary HFE-143m + HFC-125 mixture, the bubble-point pressure representation is developed almost within ±12 kPa, equivalent to the estimated experimental uncertainty.

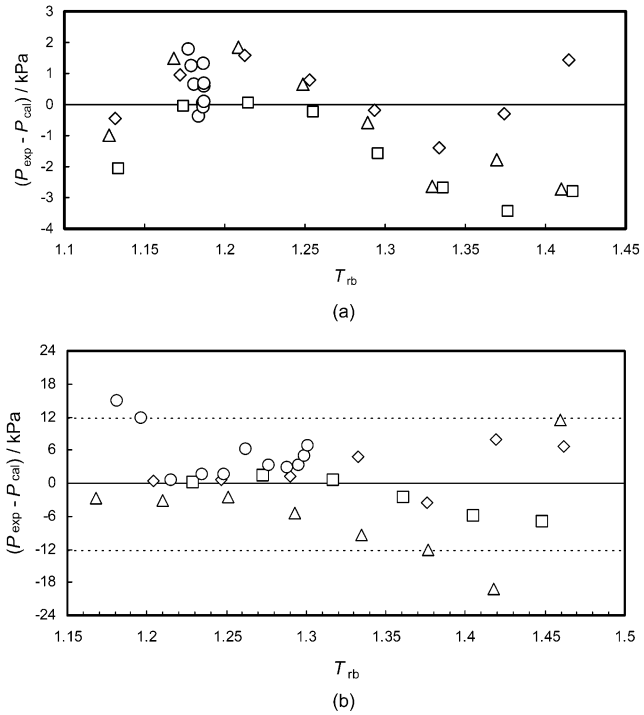

Figure 4. Deviation of the measured bubble-point pressures from the PR equation for the binary HFE-143m + HFC-134a mixture (a), and the binary HFE-143m + HFC-125 mixture (b): △, this work (0.75 mol of HFE-143m); ◇, this work (0.50 mol of HFE-143m); □, this work (0.25 mol of HFE-143m); ○, RITE.[15]

Table 5. Saturated-Liquid Densities of the Binary HFE-143m (1) + HFC-134a (2) System

x_1	T / K	ρ / kg·m^{-3}	x_1	T / K	ρ / kg·m^{-3}
0.7504	279.989	1175.5	0.5012	319.986	1059.2
0.7504	289.988	1144.5	0.5012	329.985	1013.9
0.7504	299.987	1110.3	0.5012	339.985	963.0
0.7504	309.986	1073.9	0.5012	349.984	902.8
0.7504	319.986	1034.7	0.2602	309.986	1125.8
0.7504	329.985	990.3	0.2602	319.986	1084.4
0.7504	339.985	942.3	0.2602	329.985	1037.3
0.7504	349.984	885.0	0.2602	339.985	985.6
0.7441	279.989	1176.4	0.2602	349.984	923.7
0.7441	289.988	1143.6	0.2602	359.984	844.5
0.7441	299.987	1109.6	0.2547	279.989	1236.7
0.7441	309.986	1073.6	0.2547	289.988	1202.7
0.7441	319.986	1034.5	0.2547	299.987	1165.4
0.7441	329.985	991.2	0.2547	309.986	1126.9
0.504	279.989	1204.0	0.2547	319.986	1085.2
0.504	289.988	1171.0	0.2547	329.985	1038.2
0.504	299.987	1136.5	0.2546	279.989	1237.4
0.504	309.986	1099.2	0.2546	289.988	1204.3
0.504	319.986	1059.0	0.2546	299.987	1167.0
0.504	329.985	1013.9	0.2546	309.986	1126.9
0.5012	279.989	1206.2	0.2546	319.986	1084.9
0.5012	289.988	1173.1	0.2546	329.985	1039.3
0.5012	299.987	1137.7	0.2546	339.985	986.4
0.5012	309.986	1100.0	0.2546	349.984	924.4

The saturated-liquid and compressed-liquid densities are measured at compositions of 0.25, 0.50, and 0.75 mol of HFE-143m and temperatures from (280 to 360) K in 10 K intervals for the binary HFE-143m + HFC-134a mixture, whereas they are measured from (280 to 350) K in 10 K intervals for the binary HFE-143m + HFC-125 mixture. The numerical values of the measured saturated-liquid and compressed-liquid densities are listed in Tables 5−8. Parts a and b, respectively, of Figure 5 show the distribution of the measured saturated-liquid densities of the binary HFE-143m + HFC-134a and HFE-143m + HFC-125 mixtures, respectively, in terms of saturated-liquid molar volumes. The solid lines in Figure 5 are calculated from the saturated-liquid density correlation developed in the present study, to be discussed later. Figure 5a demonstrates that at lower temperatures the saturated-liquid molar volume of the binary HFE-143m + HFC-134a mixture deviates only slightly (about 0.10 cm^3·mol^{-1} at 280 K and $x_1 = 0.25$) from the averaged saturated-liquid molar volume values of the two components, while at higher temperatures it shows a higher value than the averaged one (about 1.18 cm^3·mol^{-1} at 360 K and $x_1 = 0.25$). On the contrary, the saturated-liquid molar volumes of the binary HFE-143m + HFC-125 show smaller values than the averaged one and this tendency becomes significant at higher temperatures. Since HFC-125 has a greater saturated-liquid molar volume than that of HFE-143m at respective temperatures, the gradient of the curve in Figure 5b has an opposite sign from that in Figure 5a. The slope of the curve in Figure 5b becomes steeper with increasing temperature, especially above the critical temperature of HFC-125 (339.17 K).

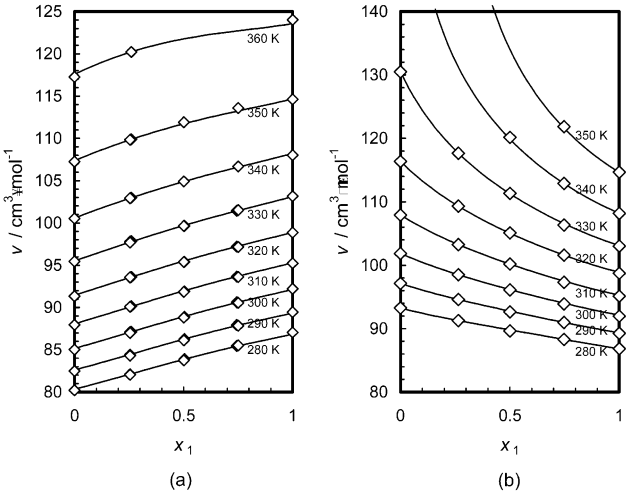

Figure 5. Distribution of the measured saturated-liquid molar volume of the binary HFE-143m + HFC-134a mixture (a), and the binary HFE-143m + HFC-125 mixture (b).

The measured saturated-liquid densities are represented by means of a correlation given in eq 4. In eq 4, ρ_s denotes the saturated-liquid density, ρ_{cm} and T_{cm} are the critical density and the critical temperature, respectively, and the subscript m denotes the mixtures. The critical temperatures and the critical densities are formulated by a correlation with a functional form given in eq 2 on the basis of the experimental data by the RITE,[15] while the exponents a_m and b_m and the coefficients A_m and B_m are determined on the basis of the present measurements also by eq 5, where L denotes any arbitrary property or parameter. The critical temperatures and critical densities of single components are listed in Table 1; the numerical values of the parameters a, b, A, and B for the pure components are given in Table 9. Cross parameters, ΔL_{ij}, in eq 5 for each property and parameter are tabulated in Table 4.

$$\frac{\rho_s}{\rho_{cm}} - 1 = A_m\left(1 - \frac{T}{T_{cm}}\right)^{a_m} + B_m\left(1 - \frac{T}{T_{cm}}\right)^{b_m} \qquad (4)$$

$$L_m = \sum L_i x_i + \sum\sum x_i x_j \Delta L_{ij} \qquad (5)$$

Equation 4 is then used in the present study to represent the measured compressed-liquid densities by means of eq

Table 6. Compressed-Liquid Densities of the Binary HFE-143m (1) + HFC-134a (2) System

x_1	T/K	P/kPa	ρ/kg·m^{-3}	x_1	T/K	P/kPa	ρ/kg·m^{-3}	x_1	T/K	P/kPa	ρ/kg·m^{-3}	x_1	T/K	P/kPa	ρ/kg·m^{-3}
0.7441	279.989	1006.9	1179.2	0.5040	289.988	2977.2	1184.4	0.7504	279.989	1017.5	1178.7	0.5012	299.987	2998.9	1151.6
0.7441	279.989	1491.2	1181.3	0.5040	299.987	996.0	1138.6	0.7504	279.989	1505.1	1181.1	0.5012	309.986	1505.2	1104.6
0.7441	279.989	2007.5	1183.3	0.5040	299.987	1515.9	1141.8	0.7504	279.989	1994.9	1183.2	0.5012	309.986	1996.1	1108.5
0.7441	279.989	2504.6	1185.1	0.5040	299.987	2032.9	1144.8	0.7504	279.989	2507.2	1184.9	0.5012	309.986	2503.2	1112.2
0.7441	279.989	3010.2	1186.6	0.5040	299.987	2502.0	1147.8	0.7504	279.989	2988.4	1186.5	0.5012	309.986	2990.5	1115.3
0.7441	289.988	489.6	1143.6	0.5040	299.987	2978.9	1150.6	0.7504	289.988	1003.3	1146.4	0.5012	319.986	1492.8	1062.1
0.7441	289.988	1007.7	1146.0	0.5040	309.986	1476.3	1104.0	0.7504	289.988	1501.1	1148.8	0.5012	319.986	1995.2	1067.6
0.7441	289.988	1508.5	1148.6	0.5040	309.986	2028.3	1107.8	0.7504	289.988	2002.4	1151.2	0.5012	319.986	2498.0	1072.0
0.7441	289.988	2009.1	1151.4	0.5040	309.986	2502.0	1111.2	0.7504	289.988	2503.1	1154.1	0.5012	319.986	3000.5	1076.4
0.7441	289.988	2507.2	1153.9	0.5040	309.986	3007.8	1114.3	0.7504	289.988	3000.4	1156.9	0.5012	329.985	2004.8	1020.7
0.7441	289.988	3004.4	1156.5	0.5040	319.986	1521.1	1062.1	0.7504	299.987	1006.8	1111.9	0.5012	329.985	2494.8	1026.8
0.7441	299.987	651.0	1109.6	0.5040	319.986	2009.9	1066.7	0.7504	299.987	1501.5	1115.4	0.5012	329.985	2981.9	1032.3
0.7441	299.987	1007.1	1112.0	0.5040	319.986	2511.1	1071.3	0.7504	299.987	2000.1	1118.2	0.5012	339.985	2505.4	974.3
0.7441	299.987	1520.9	1114.9	0.5040	319.986	2993.6	1075.5	0.7504	299.987	2502.5	1121.3	0.5012	339.985	2989.5	982.0
0.7441	299.987	2015.6	1118.2	0.5040	329.985	2002.3	1020.9	0.7504	299.987	2999.7	1123.8	0.5012	349.984	2981.4	921.6
0.7441	299.987	2505.0	1120.9	0.5040	329.985	2509.3	1025.9	0.7504	309.986	1507.0	1077.4	0.2546	279.989	999.9	1238.5
0.7441	299.987	2991.2	1123.0	0.5040	329.985	2985.7	1030.9	0.7504	309.986	2002.3	1081.8	0.2546	279.989	1504.0	1239.9
0.7441	309.986	857.9	1073.6	0.2547	279.989	1014.4	1239.0	0.7504	309.986	2503.1	1085.9	0.2546	279.989	2000.5	1241.2
0.7441	309.986	1505.7	1078.5	0.2547	279.989	1482.3	1240.4	0.7504	309.986	2997.1	1089.3	0.2546	279.989	2504.0	1243.8
0.7441	309.986	2004.5	1082.3	0.2547	279.989	1993.2	1242.0	0.7504	319.986	1504.6	1038.3	0.2546	279.989	2999.8	1246.0
0.7441	309.986	2504.5	1085.8	0.2547	279.989	2464.9	1242.6	0.7504	319.986	2003.0	1043.6	0.2546	289.988	996.1	1205.3
0.7441	309.986	3004.4	1088.9	0.2547	289.988	1007.7	1204.6	0.7504	319.986	2501.1	1047.8	0.2546	289.988	1501.0	1207.4
0.7441	319.986	1107.1	1034.5	0.2547	289.988	1517.8	1206.9	0.7504	319.986	3001.5	1052.4	0.2546	289.988	2000.9	1210.3
0.7441	319.986	1510.4	1038.4	0.2547	289.988	2031.7	1209.3	0.7504	329.985	2010.0	999.0	0.2546	289.988	2502.2	1212.0
0.7441	319.986	2010.2	1042.9	0.2547	289.988	2485.9	1211.0	0.7504	329.985	2498.3	1004.5	0.2546	289.988	3000.2	1214.2
0.7441	319.986	2500.7	1047.2	0.2547	299.987	1018.3	1167.3	0.7504	329.985	2992.1	1010.1	0.2546	299.987	999.9	1168.4
0.7441	319.986	2993.3	1051.2	0.2547	299.987	1489.5	1169.5	0.7504	339.985	2506.2	955.0	0.2546	299.987	1504.6	1171.0
0.7441	329.985	1410.3	991.2	0.2547	299.987	2001.2	1173.9	0.7504	339.985	2998.8	962.3	0.2546	299.987	2002.1	1175.7
0.7441	329.985	2010.5	998.7	0.2547	299.987	2480.5	1176.8	0.7504	349.984	2504.7	893.8	0.2546	299.987	2503.3	1177.4
0.7441	329.985	2496.6	1004.4	0.2547	309.986	1511.5	1131.4	0.7504	349.984	2993.6	905.2	0.2546	299.987	3002.7	1180.5
0.7441	329.985	2996.0	1009.6	0.2547	309.986	1985.6	1135.1	0.5012	279.989	1006.4	1208.2	0.2546	309.986	1505.6	1133.2
0.5040	279.989	984.4	1206.2	0.2547	309.986	2526.3	1138.7	0.5012	279.989	1523.5	1209.9	0.2546	309.986	2002.3	1135.3
0.5040	279.989	1502.3	1208.7	0.2547	319.986	1184.6	1085.2	0.5012	279.989	2001.4	1212.2	0.2546	309.986	2501.8	1139.2
0.5040	279.989	1987.8	1210.5	0.2547	319.986	1487.2	1087.8	0.5012	279.989	2497.5	1214.4	0.2546	309.986	3000.3	1142.3
0.5040	279.989	2559.0	1212.2	0.2547	319.986	2006.7	1093.0	0.5012	279.989	2993.6	1215.6	0.2546	319.986	1504.1	1088.2
0.5040	279.989	2950.3	1213.2	0.2547	329.985	2008.9	1044.4	0.5012	289.988	998.7	1175.9	0.2546	319.986	2001.9	1092.4
0.5040	289.988	956.3	1173.6	0.2547	329.985	2512.3	1050.6	0.5012	289.988	1496.2	1177.6	0.2546	319.986	2502.4	1097.3
0.5040	289.988	1508.7	1176.2	0.2602	339.985	2503.3	995.3	0.5012	289.988	1998.0	1180.7	0.2546	319.986	3003.4	1101.8
0.5040	289.988	2004.4	1178.6	0.2602	339.985	2994.0	1004.4	0.5012	289.988	2494.8	1182.9	0.2546	329.985	2008.9	1045.1
0.5040	289.988	2527.4	1181.7	0.2602	349.984	3008.9	940.4	0.5012	289.988	2997.1	1184.9	0.2546	329.985	2498.6	1051.2
								0.5012	299.987	1007.0	1139.5	0.2546	329.985	3002.1	1056.6
								0.5012	299.987	1499.0	1142.8	0.2546	339.985	2507.1	997.1
								0.5012	299.987	1997.4	1145.7	0.2546	339.985	2997.7	1005.5
								0.5012	299.987	2495.5	1148.7	0.2546	349.984	2994.9	941.7

Table 7. Saturated-Liquid Densities of the Binary HFE-143m (1) + HFC-125 (2) System

x_1	T/K	ρ/kg·m^{-3}	x_1	T/K	ρ/kg·m^{-3}
0.7474	279.989	1190.1	0.5008	309.986	1098.0
0.7474	289.988	1155.0	0.5008	319.986	1046.8
0.7474	299.987	1119.2	0.5008	329.985	988.2
0.7474	309.986	1079.9	0.5008	339.985	915.5
0.7474	319.986	1034.3	0.2647	279.989	1256.9
0.7474	329.985	988.1	0.2647	289.988	1212.9
0.7474	339.985	930.7	0.2647	299.987	1164.6
0.7474	349.984	862.4	0.2647	309.986	1111.3
0.5008	279.989	1227.1	0.2647	319.986	1049.6
0.5008	289.988	1187.5	0.2647	329.985	975.2
0.5008	299.987	1144.6			

6 reported elsewhere.[16] P_s in eq 6 is the bubble-point pressure that can be calculated from the PR equation discussed previously or from the bubble-point pressure correlation given in eq 7 by optimizing the acentric factor for mixtures, ω_m, on the basis of the measured bubble-point pressures. D and E in eq 6 are given in eqs 8 and 9, respectively, with $\tau = 1 - T/T_{cm}$. The acentric factor and the critical pressure for mixtures are again represented by eq 5 with the cross parameters tabulated in Table 4. The cross parameters for the critical pressures of mixtures are optimized on the basis of the data by the RITE.[15]

$$\ln \frac{\rho_s}{\rho} = E \ln\left(\frac{P + D}{P_s + D}\right) \tag{6}$$

$$\ln \frac{P_s}{P_{cm}} = 5.92715 - \frac{6.09649}{T_r} - 1.28863 \ln T_r + 0.169347 T_r^6 + \omega_m\left(13.4902 - \frac{13.8756}{T_r} - 11.1704 \ln T_r + 0.385433 T_r^6\right) \tag{7}$$

$$\frac{D}{P_{cm}} + 1 = 13.406\tau + 66.7486\tau^2 - 97.1726\tau^3 + \tau^4 \exp(-22.4997 + 226.792\omega_m - 451.956\omega_m^2) \tag{8}$$

$$E = -0.147397 + 0.1704\omega_m \tag{9}$$

Figure 6a illustrates the deviation of the measured saturated-liquid (closed symbols) and compressed-liquid (open symbols) densities of the binary HFE-143m + HFC-134a mixture from eq 6. As shown in the figure, at higher

Table 8. Compressed-Liquid Densities of the Binary HFE-143m (1) + HFC-125 (2) System

	T	P	ρ		T	P	ρ
x_1	K	kPa	kg·m^{-3}	x_1	K	kPa	kg·m^{-3}
0.7474	279.989	1006.1	1193.2	0.5008	289.988	2482.4	1199.3
0.7474	279.989	1499.9	1194.5	0.5008	289.988	2966.1	1202.1
0.7474	279.989	2002.0	1197.1	0.5008	299.987	1508.7	1148.5
0.7474	279.989	2495.2	1198.4	0.5008	299.987	1991.4	1153.9
0.7474	279.989	2989.1	1200.4	0.5008	299.987	2520.1	1157.7
0.7474	289.988	1007.2	1157.6	0.5008	299.987	2965.7	1161.3
0.7474	289.988	1509.8	1161.3	0.5008	309.986	1996.0	1106.7
0.7474	289.988	2016.2	1164.1	0.5008	309.986	2475.3	1111.6
0.7474	289.988	2507.1	1166.9	0.5008	309.986	2977.8	1117.0
0.7474	289.988	2969.1	1168.7	0.5008	319.986	1983.9	1053.0
0.7474	299.987	1494.1	1123.5	0.5008	319.986	2472.1	1059.3
0.7474	299.987	2000.3	1127.5	0.5008	319.986	2975.1	1067.5
0.7474	299.987	2489.6	1130.7	0.5008	329.985	2506.9	998.9
0.7474	299.987	2984.7	1133.9	0.5008	329.985	2977.9	1008.6
0.7474	309.986	1496.5	1083.9	0.5008	339.985	2967.2	932.3
0.7474	309.986	2010.4	1087.4	0.2647	279.989	1013.3	1262.0
0.7474	309.986	2500.3	1091.4	0.2647	279.989	1500.5	1262.9
0.7474	309.986	2954.4	1095.5	0.2647	279.989	2001.6	1266.5
0.7474	319.986	2006.3	1043.0	0.2647	279.989	2489.8	1269.2
0.7474	319.986	2482.5	1048.6	0.2647	279.989	2995.1	1272.4
0.7474	319.986	2974.2	1053.2	0.2647	289.988	1507.7	1218.5
0.7474	329.985	1980.9	991.9	0.2647	289.988	2012.7	1222.9
0.7474	329.985	2499.3	999.8	0.2647	289.988	2510.2	1226.7
0.7474	329.985	2948.9	1007.0	0.2647	289.988	2982.3	1230.9
0.7474	339.985	2492.9	940.3	0.2647	299.987	1505.2	1168.3
0.7474	339.985	2992.4	950.8	0.2647	299.987	2001.8	1173.9
0.7474	349.984	2937.1	875.3	0.2647	299.987	2499.4	1179.3
0.5008	279.989	1002.9	1228.7	0.2647	299.987	2990.3	1184.2
0.5008	279.989	1502.8	1232.8	0.2647	309.986	2006.5	1119.2
0.5008	279.989	1996.3	1235.3	0.2647	309.986	2509.7	1126.6
0.5008	279.989	2507.7	1238.0	0.2647	309.986	2983.4	1133.1
0.5008	279.989	2966.4	1239.3	0.2647	319.986	2505.6	1062.7
0.5008	289.988	1513.4	1192.6	0.2647	319.986	2987.9	1072.4
0.5008	289.988	1999.3	1196.2	0.2647	329.985	2986.5	995.4

Table 9. Parameters Used in Eqs 4 and 5

	HFC-134a	HFC-125[a]	HFE-143m
a_i	0.38	0.37	0.30
b_i	1.62	1.13	0.87
A_i	2.452 76	2.228 14	1.635 64
B_i	0.447 314	0.451 997	1.270 21

[a] Widiatmo et al.[10]

temperatures (corresponding to lower densities in the figure), eq 6 underestimates the measured densities. This may be considered due to a possible inability of the two-term eq 4, which is used as the reference standard in eq 6, to represent the measured saturated-liquid densities at high temperatures. The underestimation of compressed-liquid densities by eq 6 at lower temperatures may be due to the temperature characteristics of coefficient E in eq 5. However, except some data points at lower temperatures, a satisfactory agreement between the measured and calculated values within the estimated uncertainty, ±2.2 kg·m^{-3} shown by the dashed lines in the figure, has been obtained from eq 6. In terms of relative density deviation, the agreement was excellent within ±0.2%.

Concerning the binary HFE-143m + HFC-125 mixture, except some data points at lower temperatures, a satisfactory agreement between the measured and calculated values within the estimated uncertainty, ±2.2 kg·m^{-3} shown by the dashed lines in Figure 6b, has been obtained from eq 6. In terms of relative density deviation, the agreement was within ±0.25%. It should be noted that the bubble-point pressures calculated from the PR equation have been used as P_s in eq 6 for deriving the compressed-liquid densities in the figure. Almost similar results were confirmed when the bubble-point pressures calculated from eq 7 were used as P_s, except those at higher temperatures,

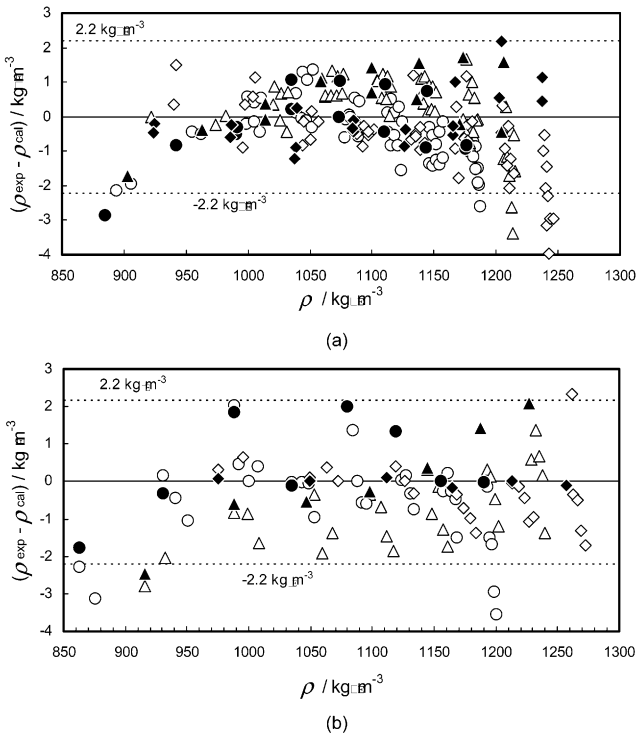

Figure 6. Deviation of the measured saturated and compressed liquid densities from eq 11 for the binary HFE-143m + HFC-134a mixture (a), and the binary HFE-143m + HFC-125 mixture (b): ●, saturated liquid (0.75 mol of HFE-143m); ○, compressed liquid (0.75 mol of HFE-143m); ▲, saturated liquid (0.50 mol of HFE-143m); △, compressed liquid (0.50 mol of HFE-143m); ◆, saturated liquid (0.25 mol of HFE-143m); ◇, compressed liquid (0.25 mol of HFE-143m).

where eq 6 overestimates the measured compressed-liquid densities by about 4 kg·m^{-3}, as a consequence of low bubble-point pressure representation by eq 7.

Conclusions

The bubble-point pressures and liquid densities of the binary HFC-134a + HFE-143m and HFC-125 + HFE-143m mixtures have been measured at temperatures from (280 to 360) K and mole fractions of 0.25, 0.50, and 0.75 HFE-143m as the first component. On the basis of the measured bubble-point pressures, the PR equation has been optimized to lead to the data representation within the estimated experimental uncertainty. The saturated-liquid density correlation has also been developed so as to provide reference density values for the proposed compressed-liquid density correlation, which allows liquid density representation within ±2.2 kg·m^{-3}.

Literature Cited

(1) Wang, B. H.; Adcock, J. L.; Mathur, S. B.; van Hook, W. A. Vapor Pressures, Liquid Molar Volumes, Vapor Nonidealities, and Critical Properties of Some Fluorinated Ethers: $CF_3OCF_2OCF_3$, $CF_3OCF_2CF_2H$, c-$CF_2CF_2CF_2O$, CF_3OCF_2H, and CF_3OCH_3; and of CCl_3F and CF_2ClH. *J. Chem. Thermodyn.* **1991**, *23*, 699−710.

(2) Salvi-Narkhede, M.; Wang, B. H.; Adcock, J. L.; van Hook, W. A. Vapor Pressures, Liquid Molar Volumes, Vapor Nonidealities, and Critical Properties of Some Partially Fluorinated Ethers (CF_3-OCF_2CF_2H, CF_3OCF_2H, and CF_3OCH_3), Some Perfluoroethers ($CF_3OCF_2OCF_3$, c-$CF_2OCF_2OCF_2$, and c-$CF_2CF_2CF_2O$), and of CHF_2Br and CF_3CFHCF_3. *J. Chem. Thermodyn.* **1992**, *24*, 1065−1075.

(3) Sako, T.; Sato, M.; Nakazawa, N.; Oowa, M.; Sekiya, A.; Ito, H.; Yamashita, S. Thermodynamic Properties of Fluorinated Ethers as Alternative Refrigerants. *Proc. Joint Meeting of IIR Commissions, CFCs, The Day After*, 1994, Padova, Italy; pp 485−491.

(4) Sako, T.; Sato, M.; Nakazawa, N.; Oowa, M.; Yasumoto, M.; Ito, H.; Yamashita, S. Critical Properties of Fluorinated Ethers. *J. Chem. Eng. Data* **1996**, *41*, 802−805.
(5) Beyerlein, A. L.; DesMarteau, D. D.; Kul, I.; Zhao, G. Properties of Novel Fluorinated Compounds and Their Mixtures as Alternative Refrigerants. *Fluid Phase Equilib.* **1998**, *150*−*151*, 287−296.
(6) Kul, I.; DesMarteau, D. D.; Beyerlein, A. L. Vapor-Liquid Equilibrium and Densities of RE-143a (CF_3OCH_3)/RE-218 (CF_3OCF_2-CF_3) Mixtures as R-12 or R-22 Alternatives. *ASHRAE Trans.* **2000**, *106* (Part 1), 351−357.
(7) Kul, I.; DesMarteau, D. D.; Beyerlein, A. L. Vapor-liquid Equilibria for CF_3OCF_2H/Fluorinated Ethane and CF_3SF_5/Fluorinated Ethane Mixtures as Potential R-22 Alternatives. *Fluid Phase Equilib.* **2001**, *185* (1−2), 241−253.
(8) Yamada, Y.; Kondo, S.; Maruo, K.; Sekiya, A. Hydrofluoroethers as Alternative Refrigerants. *13th European Symposium on Fluorine Chemistry*, July 17, 2001, Bordeaux, France; poster 1P-70.
(9) Peng, D. Y.; Robinson, D. B. A New Two-Constant Equation of State. *Ind. Eng. Chem. Fundam.* **1976**, *15* (1), 59−64.
(10) Widiatmo, J. V.; Fujimine, T.; Sato, H.; Watanabe, K. Liquid Densities of Alternative Refrigerants Blended with Difluoromethane, Pentafluoroethane, and 1,1,1,2-Tetrafluoroethane. *J. Chem. Eng. Data* **1997**, *42*, 270−277.
(11) Yoshii, Y.; Widiatmo, J. V.; Watanabe, K. Measurements of Critical Parameters for HFE-143m. *Rev. High Pressure Sci. Technol.* **2000**, *10*, 247 (in Japanese).
(12) Widiatmo, J. V.; Watanabe, K. Equations of State for Fluorinated Ether Refrigerants, CF3OCH3 and (CF3)2CFOCH3. *Proc. IIR Conf., Thermophys. Prop. and Transfer Processes of New Refrigerants*, October 3−5, 2001, Paderborn, Germany.
(13) Widiatmo, J. V.; Sato, H.; Watanabe, K. Saturated-liquid Densities and Bubble-point Pressures of Binary System HFC-32 + HFC-125. *High Temp.*−*High Pressures* **1993**, *25*, 677−683.
(14) International Organization of Standardization. *Guide to the Expression of Uncertainty in Measurement*; ISO: Switzerland, 1993.
(15) Yasumoto, M., Research Institute of Innovative Technology for the Earth (RITE), Tsukuba, Japan, personal communications, 2001.
(16) Widiatmo, J. V.; Fujimine, T.; Sato, H.; Watanabe, K. Bubble-Point Pressures and Liquid Densities of Mixtures Blended with Difluoromethane, Pentafluoroethane, and 1,1,1-Trifluoroethane. *J. Chem. Eng. Data* **1999**, *44*, 1315−1320.

Received for review March 26, 2002. Accepted June 28, 2002. The present study was partially supported by the New Energy Development Organization (NEDO) through the RITE, and the authors are grateful to these organizations.

JE020055B